JOURNAL OF CATALYSIS 37, 223–231 (1975)

Oxidation of Propene in the Absence of Gaseous Oxygen

II. Bismuth Molybdates and Iron Antimonates

VITTORIO FATTORE, ZYGMUNT A. FUHRMAN, GIOVANNI MANARA
AND BRUNO NOTARI

Snamprogetti S.p.A., Direzione Ricerca e Sviluppo,
San Donato Milanese, Italy

Received February 13, 1974; revised October 1, 1974

Propene oxidation in the absence of gaseous oxygen has been studied on unsupported bismuth molybdate with atomic ratio Mo/Bi = 2.66, and on unsupported iron antimonates prepared according to various procedures. The study was carried out in a flow reactor: the distribution of the products and the oxygen consumption were followed. The experimental conditions were: temperature, 450–550°C; C_3H_6 WHSV, 0.1–0.2 hr^{-1}; and C_3H_6 partial pressure, 108 mbar.

On bismuth molybdate and iron antimonate with ratio Sb/Fe = 2 the main oxidation product was acrolein, whereas for Sb/Fe = 1 deep oxidation products were obtained. The structural modifications occurring during the reduction of bismuth molybdate are pointed out and the structure of the intermediate phase was elucidated. The chemical composition of this intermediate is close to $2Bi_2O_3 \cdot MoO_3$ and the structure is monoclinic pseudo-tetragonal ($a = b = 5.58$ Å; $c = 11.62$ Å; $\gamma = 89.00°$). The different behavior of iron–antimony catalysts obtained varying the chemical composition and the thermal treatment of the samples supports the hypothesis that the two phases of the catalyst, $FeSbO_4$ and Sb_2O_4, cooperate in producing acrolein with a higher selectivity than on each phase alone. A mechanism has been proposed to explain the phenomenon.

INTRODUCTION

Many oxide-based compositions are successfully adopted for the selective heterogeneous oxidation and/or ammoxidation of olefins, antimony or molybdenum being present in the majority of them. Among them it is evident that the iron–antimony system is far less studied (*1–4*) in comparison to other catalysts. The present research was undertaken to achieve a better knowledge of this catalyst and to investigate whether the optimum catalytic activity can be related to some peculiar feature of the solid. We thought a comparison between the Fe_2O_3–Sb_2O_4 system and the Bi_2O_3–MoO_3 system would be of great interest. The latter system has stimulated in recent years extensive investigations on physicochemical properties in correlation with catalytic activity and selectivity (*5–10*). We chose to oxidize propene (PR) on both catalysts, in depletive conditions, that is to utilize the lattice oxygen as the oxidizing species and to measure the change of catalytic activity and product distribution as a function of the increasing degree of reduction of the solid.

In Part I (*11*) we studied under the same conditions the behavior of the simple antimony, bismuth, iron and molybdenum oxides. Iron oxide proved very active and not selective and underwent a complete transformation to Fe_3O_4; antimony oxide, on the other hand, showed low activity but high selectivity, 1-5-hexadiene (HEX) being the main partial oxidation product. In the last case the oxygen consumed was predominantly supplied by the surface. MoO_3 and Bi_2O_3 were both active and selective, the former producing mainly acrolein (ACR) and the latter benzene (BEN), with a great mobility and a noticeable consumption of the bulk oxygen, even though X-ray analysis detected only small structural modifications.

The present investigation was undertaken to investigate the extent to which the behavior of the simple oxides could provide explanations and suggestions for the interpretation of the performances obtained with the systems Fe_2O_3–Sb_2O_4 and Bi_2O_3–MoO_3.

EXPERIMENTAL METHODS

The catalysts were prepared according to the following procedure:

MoBi. The bismuth molybdate unsupported catalyst (MoBi) was prepared by slowly adding at room temperature a solution of $Bi(NO_3)_3 \cdot 5H_2O$ in dilute nitric acid to an ammonia solution of $(NH_4)_6Mo_7O_{24} \cdot 4H_2O$. The final pH was 2.2. After drying, the powder was pelletized and activated in air up to 600°C. The composition of the final product was $Bi_2O_3 \cdot 2.66\ MoO_3$ and its BET surface area was 3.3 $m^2\ g^{-1}$.

FeSb 1 and FeSb 2. The samples with atomic ratio Sb/Fe = 1 (FeSb 1) and Sb/Fe = 2 (FeSb 2) were prepared by heating at 80°C the desired amount of $Fe(NO_3)_3 \cdot 9H_2O$ which melts in its hydration water giving a concentrated solution of $Fe(NO_3)_3$. The corresponding amount of finely divided Sb_2O_3 was added to this solution, and the resulting slurry was carefully stirred. The mixture was then evaporated and the powder obtained was activated up to 800°C. The surface area of the final products was 28 $m^2\ g^{-1}$ for FeSb 1 and 13 $m^2\ g^{-1}$ for FeSb 2.

MIX 1. FeSb 1 and Sb_2O_4 were separately calcined at 800°C for 2 hr and subsequently mixed together in such a ratio as to obtain Sb/Fe = 2.

MIX 2. This was prepared by calcining MIX 1 at 800°C for 2 hr.

The final products were pelletized, ground and sieved: the fraction between 50 to 70 mesh was collected for the experiments.

The reagents, equipment, analytical and operative procedure and nomenclature have been described and defined in Part I (*11*).

The particular operating conditions chosen for the experiments to be described below were: temperature, 450–550°C; reduction time t_r, 1–20 min; C_3H_6 partial pressure, 108 mbar; C_3H_6 weight hourly space velocity, WHSV, 0.1–0.2 hr^{-1}.

RESULTS

Conversion and Selectivity

Propene conversions against reduction time, t_r, at 450 and 550°C are plotted in Figs. 1 and 2 for all the investigated solids. The initial conversion is nearly 100% in all cases except MoBi at 450°C and sharply decreases towards 10–20% after a few minutes of reduction. At 550°C the behav-

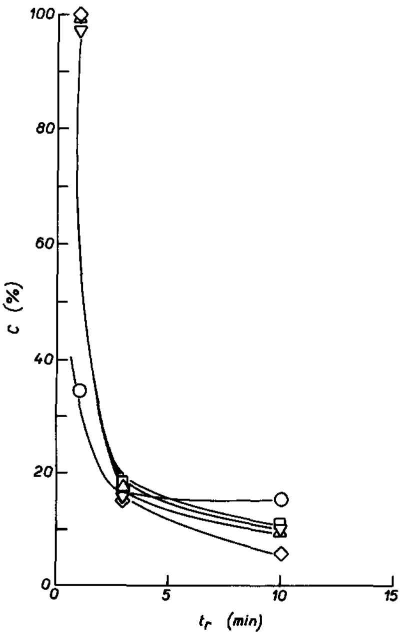

FIG. 1. Values of the conversion of PR versus t_r at 450°C: (◇)FeSb 1, (□)FeSb 2, (▽)MIX 1, (△)MIX 2, (○)MoBi.

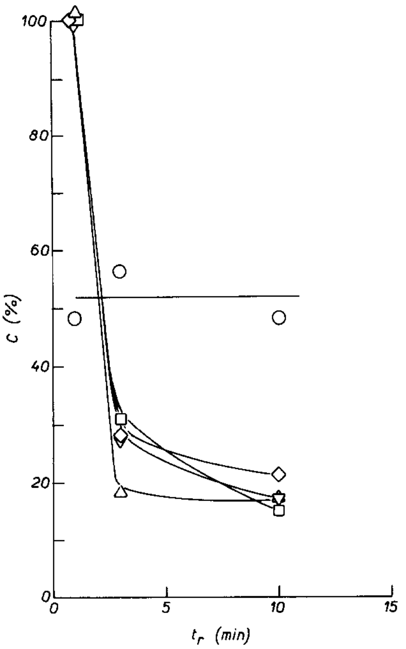

FIG. 2. Values of the conversion of PR vs t_r at 550°C: (◇)FeSb 1, (□)FeSb 2, (▽)MIX 1, (△)MIX 2, (○)MoBi.

ior is quite similar for all solids, with exception made again for MoBi. Propene conversions around 50%, nearly independent of the degree of reduction, are obtained on this catalyst.

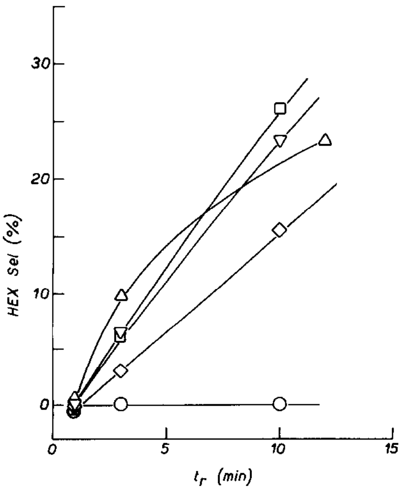

FIG. 3. Values of selectivity to HEX versus t_r at 550°C: (◇)FeSb 1, (□)FeSb 2, (▽)MIX 1, (△)MIX 2, (○)MoBi.

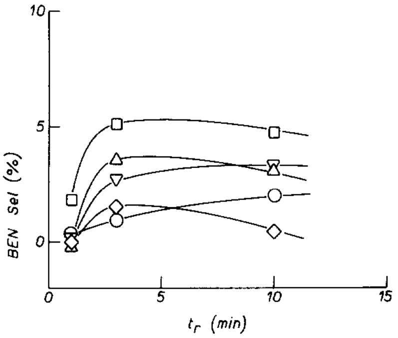

FIG. 4. Values of selectivity to BEN versus t_r at 550°C: (◇)FeSb 1, (□)FeSb 2, (▽)MIX 1, (△)MIX 2, (○)MoBi.

The selectivities to the main oxidation products at 550°C, and in the case of ACR also at 450°C, are plotted against the reduction time in Figs. 3–6. It may be noticed that HEX is not produced on MoBi in the temperature range we considered; on the iron–antimony catalysts the amount of HEX increases almost linearly with t_r and is nearly independent of the temperature. BEN production is low on every catalyst (less than 5%) and is independent of t_r and temperature. The selectivity to ACR on MoBi is extremely high, around

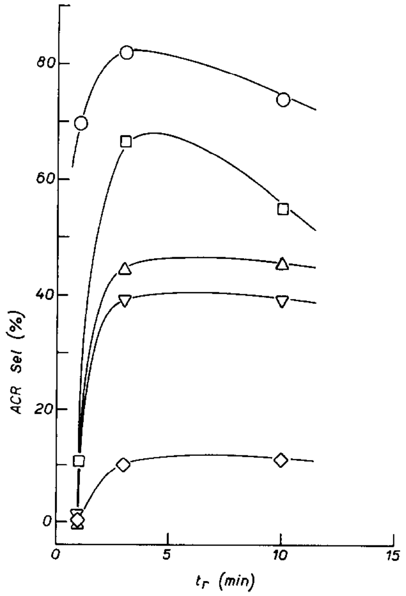

FIG. 5. Values of selectivity to ACR versus t_r at 450°C: (◇)FeSb 1, (□)FeSb 2, (▽)MIX 1, (△)MIX 2, (○)MoBi.

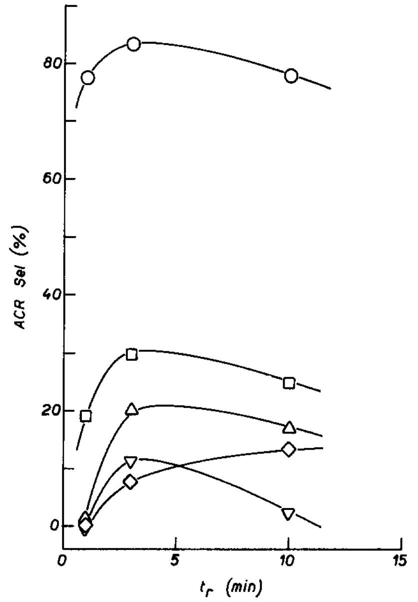

FIG. 6. Values of selectivity to ACR versus t_r at 550°C: (◇)FeSb 1, (□)FeSb 2, (▽)MIX 1, (△)MIX 2, (○)MoBi.

80%, and does not change with temperature. The significant behavior of the iron–antimony catalysts must be accurately examined. The selectivity to ACR on FeSb 1 is low, and nearly constant with temperature; on the other hand, on FeSb 2 the selectivity at 450°C is almost as high as on MoBi, but it decreases sharply as the temperature is increased. MIX 1 and MIX 2 are both more selective than FeSb 1 and less selective than FeSb 2. The selectivity to ACR follows the order MoBi > FeSb 2 > MIX 2 > MIX 1 > FeSb 1; its dependence on the reduction time is nearly the same, showing a maximum after 3 min of reduction and then a slow decrease. On raising the temperature, CO and CO_2 increase on all the iron–antimony catalysts. The difference between the various iron–antimony catalysts is evident only after the first minute, because at the beginning they behave in quite identical ways producing predominantly CO and CO_2; afterwards they sharply differ among themselves.

Catalyst Structure

FeSb 1. The structure determined by X-ray analysis (see Table 1) agrees with the one proposed in the literature (*12,13*), where a tetragonal phase with a rutile-type structure and a composition $FeSbO_4$ is described. By reducing with PR, for the time we considered in the experiments, no change was detectable by X-ray analysis, whereas, when the reduction was protracted for longer periods (up to 1 hr), a decomposition of the rutile phase was evident with formation of large amounts of β-Sb_2O_4 and traces of α-Sb_2O_4. Such a decomposition must run parallel to the formation of iron oxide, but this phase was not detected by X-ray analysis.

FeSb 2. For this composition, the presence of two phases Sb_2O_4 and $FeSbO_4$ was reported (*1,3*), and the catalytic activity was attributed to $FeSbO_4$. For this composition, however, Adamiya *et al.* (*4*) detected an ir absorption band that they ascribed to a phase consisting of a solid solution of Sb_2O_4 and $FeSbO_4$. We examined FeSb 2 by X-rays and detected the two phases α-Sb_2O_4 and $FeSbO_4$, rutile type. Magnetic susceptibility measurements were performed on FeSb 1, FeSb 2 and on other samples with an atomic ratio

TABLE 1
PHASE COMPOSITION ACCORDING TO X-RAY ANALYSIS[a]

Reduction (min)		
	FeSb 1	
Before		$FeSbO_4$
10		$FeSbO_4$
60		$FeSbO_4$ + β-Sb_2O_4 + [α-Sb_2O_4]
	FeSb 2	
Before		$FeSbO_4$ + α-Sb_2O_4
10		$FeSbO_4$ + α-Sb_2O_4
30		$FeSbO_4$ + α-Sb_2O_4 + [β-Sb_2O_4]
60		$FeSbO_4$ + α-Sb_2O_4 + β-Sb_2O_4

[a] Brackets indicate small amounts or traces of the compound.

Sb/Fe ranging between 1 and 2.5. A constant value of magnetic susceptibility per mole of iron was obtained at room temperature, indicating that iron atoms are in the same oxidation state in all samples and their environment does not change.

In the case of FeSb 2, no structural changes are detectable by X-ray analysis during the first 10 min of reduction, whereas, when the treatment is protracted, large amounts of β-Sb_2O_4 are produced: the formation of β-Sb_2O_4 must be ascribed to the decomposition of $FeSbO_4$ and not to the transformation of α-Sb_2O_4, which remains unaffected (Table 1).

MoBi. The Bi_2O_3–MoO_3 system has been widely investigated. Even though there are discrepancies among the various authors, a substantial agreement exists about the phases with high molybdenum content $Bi_2O_3 \cdot 3MoO_3$ (*7,14*) and $Bi_2O_3 \cdot 2MoO_3$ (*7*). Two phases are reported for $Bi_2O_3 \cdot MoO_3$, the K phase, orthorhombic with koechlinitic structure (*15*) and the K II phase, stable at high temperature, with a tetragonal structure (*16*). All the above phases are described as catalytically active. Among the compositions with high bismuth content, a $2Bi_2O_3 \cdot MoO_3$ phase, which has an oxygen-deficient CaF_2 structure with a = 5.65 Å, is reported (*17*). At 870°C this cubic structure transforms into a tetragonal one. The compound $3Bi_2O_3 \cdot MoO_3$ is reported (*5,18*) to change its diffraction pattern with temperature and at 1000°C, closely resembles K II.

According to Rashkin and Pierron (*8*), who studied the structure of the $Bi_2O_3 \cdot 2MoO_3$ composition on alumina by means of high temperature diffraction, the X-ray data obtained at room temperature do not present an adequate picture of the situation at reaction temperatures. In the presence of air and PR they detected an unknown structure but it was impossible to identify it, due to the small number of observed diffraction peaks. $Bi_2O_3 \cdot MoO_3$ K and crystalline MoO_3, according to Dalin *et al.* (*19*), are the products formed from $Bi_2O_3 \cdot 2MoO_3$ and $Bi_2O_3 \cdot 3MoO_3$ after prolonged use as catalysts in the oxidative ammonolysis of PR at 470°C. Aykan (*10*), reacting PR and ammonia in the absence of gaseous oxygen on the phase $Bi_2O_3 \cdot 3MoO_3$, found that metallic bismuth and MoO_2 are the final reduction products, which would be formed through the intermediate $Bi_2O_3 \cdot MoO_3$ K. Tsailingol'd *et al.* (*24*), on the other hand, studying the oxidative dehydrogenation of *n*-butenes in the absence of gaseous oxygen on bismuth molybdates, found that the reduction of the catalyst proceeds to metallic Bi and Mo_2O_3 as the final products. However, the X-ray diffraction pattern they reported for Mo_2O_3 is identical to the ASTM pattern of MoO_2 (in ASTM the pattern of Mo_2O_3 is not reported). Our catalyst, MoBi, was composed of the phase $Bi_2O_3 \cdot 3MoO_3$ with small amounts of the phase $Bi_2O_3 \cdot MoO_3$ K. The phase modifications occurring during the reduction by PR are displayed in Fig. 7 which shows the phase composition as a function of t_r. The phase K is not

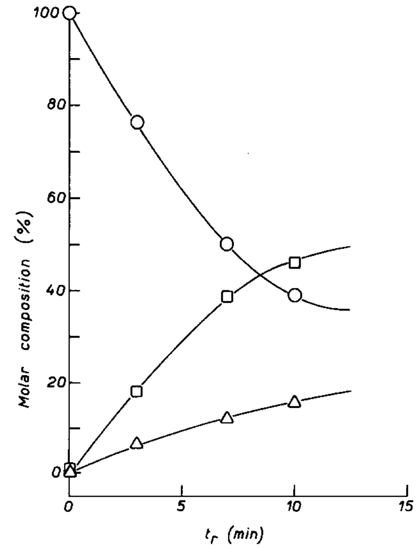

FIG. 7. Molar composition of MoBi versus t_r at 550°C: (○)$Bi_2O_3 \cdot 3MoO_3$, (□)PTPh, (△)MoO_2.

TABLE 2
X-Ray Data of PTPh[a]

d (Å)	hkl	Intensity
3.284	$\bar{1}$ 1 2	s
3.242	1 1 2	s
2.903	0 0 4	mw
2.791	200–020	ms
2.012	204–024	ms
1.738	$\bar{1}$16–116	w

[a] Unit cell parameters: a = 5.58 Å; b = 5.58 Å; c = 11.62 Å; γ = 89.00°; V = 362 Å^3.

considered because it cannot be detected any more on the reduced catalyst. The metallic Bi which should accompany the reduction was not observed by microscopic inspection of the catalyst reduced for up to 10 min, but it could be observed after extended reduction, when all the structure collapsed forming MoO_2 and Bi.

A new phase (PTPh), not before identified, was detected and partially characterized (*20*). Its chemical composition is close to that of the phase $2Bi_2O_3 \cdot MoO_3$, but it has a pseudo-tetragonal monoclinic structure; some crystal data are given in Table 2. We suggest that PTPh, which has a high bismuth content and is probably oxygen deficient, could be the intermediate formed in the reduction of bismuth molybdates. PTPh is probably the "unknown phase" detected by Aykan (*10*) and the phase whose pattern, according Batist *et al.* (*5*), closely resembles that of K II.

DISCUSSION

In Part I (*11*), we pointed out the different catalytic behavior of bismuth, molybdenum, antimony, iron and tin oxides both for activity and for the distribution of allylic products.

The behavior of MoBi and FeSb 2, which more closely resemble some industrial catalysts, is quite different from that of their constituent oxides: ACR is always the main partial oxidation product on these catalysts. Considering the number of oxygen layers consumed during the reaction as a function of t_r (Fig. 8) it is evident that the surface monolayer is consumed in the first minute. Afterwards the rate of OC remains unchanged for MoBi, whereas it decreases for FeSb 2 (and FeSb 1), whose activity is greatly dependent on the reduction (compare with Fig. 2). The linear trend of MoBi is similar to that of MoO_3 and Bi_2O_3, but with a lower OC, and the behavior of FeSb 2 and FeSb 1 is intermediate between that of their component oxides. The low influence of t_r on conversion confirms the high mobility, in reaction conditions, of lattice oxygen of MoBi (*6,21*), whereas for iron–antimony catalysts the diffusion from bulk to the surface is slower (even though faster than on Sb_2O_4).

As already pointed out, the PR oxidation is directed towards ACR, whereas the dimerization and/or cyclization of the allyl radicals are always negligible at low t_r and become significant at high t_r.

The trend of ACR selectivity versus t_r showing a maximum on the slightly re-

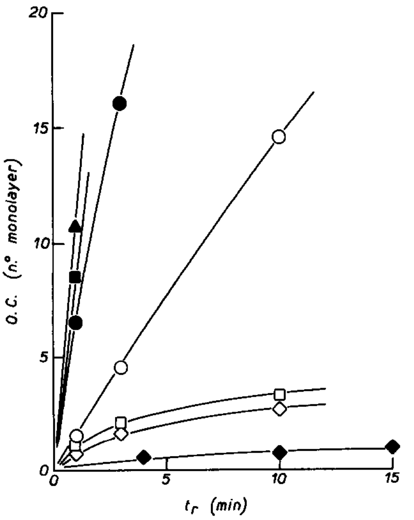

Fig. 8. Values of oxygen consumption versus t_r at 550°C: (◇)FeSb 1, (□)FeSb 2, (○)MoBi, (●)Bi_2O_3, (■)MoO_3, (▲)Fe_2O_3, (◆)Sb_2O_4.

duced catalysts suggests that industrial operating conditions in the presence of air should be selected in such a way as to allow the catalyst to work in a slightly reduced steady state, as confirmed by Dulin *et al.* (*25*) on the basis of energetic considerations.

The iron–antimony system must be carefully examined both from the catalytic and structural point of view.

Gel'bshtein *et al.* (*22*) found for a ratio Sb/Fe near to 2 a change of the activation energy for the isotopic oxygen exchange, the electron work function and the electrical conductance. Shchukin *et al.* (*23*) showed a maximum selectivity in the dehydrogenation of butenes for catalysts with an atomic ratio Sb/Fe near to 2 and ascribed this selective behavior to the phase $FeSbO_4$. However, by ir analysis Adamiya *et al.* (*4*) detected in samples with atomic ratio Sb/Fe = 2 an absorption band ascribed to a phase consisting of a solid solution of Sb_2O_4 and $FeSbO_4$. By X-ray analysis we detected only a phase $FeSbO_4$ and our measurements of magnetic susceptibility did not allow us to detect any change of the iron valence in the range of atomic ratio Sb/Fe between 1 and 2.5. The peculiar behavior corresponding to the ratio Sb/Fe = 2 could be ascribed to the hypothetical phase of Adamiya *et al.* or to a simple additivity of the separated oxides. Simple mechanical mixtures of $FeSbO_4$ and Sb_2O_4 (MIX 1 and MIX 2) produce ACR with selectivities of about 40%, much higher than any of the constituents.

This result can only be understood if it is assumed that the two separated oxides perform different functions in the sequence of a polystep reaction, and that each solid performs one of the steps in a more efficient way. Also, some kind of migration either of an intermediate product formed at the surface of one of the solids or of oxygen ions through the boundaries where the two solids are in contact must be assumed to rationalize the fact that a major reaction product (ACR) is obtained which cannot be produced by either solid alone. Since, on Sb_2O_4 products from the dimerization of allyl radicals are obtained, while on $FeSbO_4$ only traces of allyl radical derivatives are observed, it seems reasonable to postulate that allyl radical formation takes place on Sb_2O_4. Subsequently allyl radicals could migrate from Sb_2O_4 to $FeSbO_4$ via surface or gas phase, or alternatively their oxidation could be performed by oxygen ions migrating from $FeSbO_4$ to Sb_2O_4. Due to the fact that on $FeSbO_4$ there is a high probability for an organic fragment to be oxidized to CO and CO_2, it seems more reasonable to postulate that oxygen ions migrate from $FeSbO_4$ to Sb_2O_4. An atomic ratio Sb/Fe near to 2 should be reached in order to allow the catalytic behavior induced by Sb_2O_4 on $FeSbO_4$ to take place, thereby changing the reaction path occurring on $FeSbO_4$ alone.

In the light of this hypothesis, in MIX 1 allyl radicals would be formed on Sb_2O_4: however, instead of dimerizing to HEX, such radicals would form ACR due to a reaction with oxygen ions which are available as a consequence of inter-particle migration from $FeSbO_4$ to Sb_2O_4.

In catalysts working in the presence of air, the restoration of the oxygen content of $FeSbO_4$ could be obtained by reaction with gas-phase oxygen, thus reconstituting a steady state catalytic composition.

The ability of $FeSbO_4$ to release oxygen is supported by the X-ray analysis of FeSb 1 after different reduction periods, which shows the decomposition of the solid with formation of Sb_2O_4; the oxygen released requires the reduction of a species, in this case Sb^V. At the same time the production of HEX on FeSb 1 increases remarkably with the reduction, thus resembling the behavior of Sb_2O_4 alone, and suggesting the formation of Sb_2O_4 on the surface.

According to this hypothesis, FeSb 2

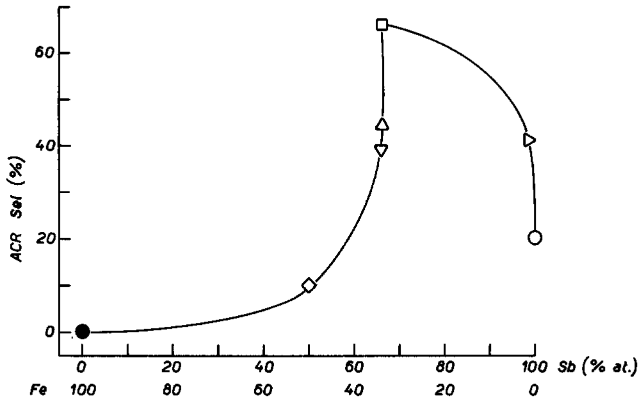

FIG. 9. Values of selectivity to ACR versus chemical composition: (◇)FeSb 1, (□)FeSb 2, (▽)MIX 1, (△)MIX 2, (▷)Sb_2O_4 + 1% at Fe, (●)Fe_2O_3, (○)Sb_2O_4.

should be nothing else but a "well dispersed" mixture of $FeSbO_4$ and Sb_2O_4: it would differ from MIX 1, the mechanical mixture of $FeSbO_4$ and Sb_2O_4, only in the degree of contact and subdivision of the constituent solid particles.

In order to check whether the higher selectivity to ACR of FeSb 2 could be ascribed to a solid solution formed at the contact points between the particles of Sb_2O_4 and $FeSbO_4$, the sintering of MIX 1 was conducted in order to increase the contact necks. The catalyst thus obtained, MIX 2, gave a slightly higher selectivity to ACR (43% against 39%), a difference which does not seem relevant to justify the role of the solid solution in the overall catalytic process.

A further experiment was performed preparing a catalyst according to the procedure followed for FeSb 2 but containing Sb and Fe in a 99:1 atomic ratio. Production of ACR was similar to the one obtained on MIX 1 and MIX 2, as shown in Fig. 9, confirming the shift from dimers (pure Sb_2O_4) to ACR as an effect of the presence of even small amounts of $FeSbO_4$ (X-ray analysis, because of the small amount of iron, could not detect any change in the pattern of Sb_2O_4 so doped).

In conclusion:

a. The existence of a new phase not before identified, formed during the reduction of bismuth molybdates, was demonstrated. This phase, with a chemical composition close to $2Bi_2O_3 \cdot MoO_3$ and a pseudotetragonal monoclinic structure, could be the intermediate formed in the reduction of bismuth molybdates.

b. The catalytic behavior of the constituent oxides cannot allow one to forecast the properties of the molybdenum–bismuth and iron–antimony catalysts.

c. The behavior of iron–antimony catalysts prepared in different ways suggests the hypothesis that the two phases of the catalyst, $FeSbO_4$ and Sb_2O_4, cooperate in producing ACR with a higher selectivity than on each phase alone.

ACKNOWLEDGMENTS

The authors thank Professor M. Cesari, Dr. G. Perego and Dr. A. Zazzetta for X-ray analyses, magnetic susceptibility measurements and for fruitful discussion concerning the structure of the catalysts.

REFERENCES

1. Vekemans, J., Walravens, J., Lambert, P., and Van Eygen, C., *Ind. Chim. Belg.* **32**, spec. number, P.2, 694 (1967).
2. Shchukin, V. P., Ven'yaminov, S. A., and Boreskov, G. K., *Kinet. Katal.* **11**, 1236 (1970).
3. Boreskov, G. K., Ven'yaminov, S. A., Dzisko, V. A., Tarasova, D. V., Dindoin, V. M., Sa-

zonova, N. N., Olen'kova, I. P., and Kefeli, L. M., *Kinet. Katal.* **10,** 1350 (1969).

4. Adamiya, T. V., Mishchenko, Y. A., Dulin, D. A., and Gel'bshtein, A. I., *Kinet. Katal.* **11,** 1168 (1970).
5. Batist, P. A., Der Kinderen, A. H. W. M., Leeuwenburgh, Y., Metz, F. A. M. G., and Schuit, G. C. A., *J. Catal.* **12,** 45 (1968).
6. Keulks, G. W., *J. Catal.* **19,** 232 (1970).
7. Erman, L. Y., Gal'perin, E. L., Kolchin, I. K., Dobrzhanskii, G. F., and Chernyshev, K. S., *Z. Neorgan. Khim.* **9,** 2174 (1964).
8. Rashkin, J. A., and Pierron, E. D., *J. Catal.* **6,** 332 (1966).
9. Batist, P. A., Kapteijns, C. J., Lippens, B. C., and Schuit, G. C. A., *J. Catal.* **7,** 33 (1967).
10. Aykan, K., *J. Catal.* **12,** 281 (1968).
11. Fattore V., Fuhrman Z. A., Manara G., and Notari, B., *J. Catal.* **37,** 215 (1975).
12. Mason, V., and Vitaliano, V., *Mineral. Mag.* **30,** 107 (1953).
13. Brandt, K., *Ark. Kemi, Mineral. Geol.* **17A,** 1 (1943).
14. Cesari, M., Perego, G., Zazzetta, A., Manara, G., and Notari, B., *J. Inorg. Nucl. Chem.* **33,** 3595 (1971).
15. Zemann, J., *Heidelberg. Beitr. Mineral. Petrogr.* **5,** 139 (1956).
16. Blasse, G., *J. Inorg. Nucl. Chem.* **28,** 1124 (1966).
17. Gattow, G., *Z. Anorg. Allgem. Chem.* **298,** 64 (1959).
18. Bleijenberg, A. C. A. M., Lippens, B. C., and Schuit, G. C. A., *J. Catal.* **4,** 581 (1965).
19. Dalin, M. A., Mangasaryan, N. A., Serebryakov, B. R., Mekhtieva, V. L., Portyanskii, A. E., and Mekhtiev, K. M., *Dokl. Akad. Nauk SSSR* **200,** 624 (1971).
20. Cesari, M., and Perego, G., private communication.
21. Adamiya, T. V., Mishchenko, Y. A., and Gel'bshtein A. I., *Kinet. Katal.* **11,** 734 (1970).
22. Gel'bshtein, A. I., Stroeva, S. S., Bakshi, Y. M., and Mishchenko, Y. A., *Proc. Int. Congr. Catal., 4th* (Moscow) *1968* **1,** 385.
23. Shchukin, V. P., Boreskov, G. K., Ven'yaminov, S. A., and Tarasova, D. V., *Kinet. Katal.* **11,** 153 (1970).
24. Tsailingol'd, A. L., Komarovskii, N. A., Chekhov, E. E., Stepanov, G. A., Tuktarova, L. S., Pankrat'ev, Y. D., and Slin'ko, M. G., *Kinet. Katal.* **13,** 1181 (1972).
25. Dulin, D. A., Airepetova, R. P., Kolabanovskaya, E. I., Parfenov, A. N., Stroeva, S. S., and Gel'bshtein, A. I., *Kinet. Katal.* **12,** 953 (1971).